AGU ADVANCING EARTH AND SPACE SCIENCES

Water Resources Research

RESEARCH ARTICLE
10.1029/2025WR040690

# Hydrodynamic Responses of Fish Community Dynamics in Large-Scale Morphologically Complex River Systems

Jiajian Qiu[1], Saiyu Yuan[1,2], Hongwu Tang[1,2], Yilin Deng[1], and Carlo Gualtieri[3]

[1]The National Key Laboratory of Water Disaster Prevention, Hohai University, Nanjing, China, [2]Key Laboratory of Hydrologic-cycle and Hydrodynamic System of Ministry of Water Resources, Hohai University, Nanjing, China, [3]Department of Structures for Engineering and Architecture, University of Napoli Federico II, Napoli, Italy

**Key Points:**

- High fish distribution heterogeneity was observed in a large river with complex channel morphologies, including narrowing and confluences
- A distinct Confluence Hydro-Ecological Zone (CHEZ) was identified, characterized by notably elevated fish density and species diversity
- CHEZ's extent and effect are governed by momentum and water-quality contrasts, as well as mixing dynamics between the converging flows

**Correspondence to:**
S. Yuan,
yuansaiyu@hhu.edu.cn

**Citation:**
Qiu, J., Yuan, S., Tang, H., Deng, Y., & Gualtieri, C. (2025). Hydrodynamic responses of fish community dynamics in large-scale morphologically complex river systems. *Water Resources Research*, *61*, e2025WR040690. https://doi.org/10.1029/2025WR040690

Received 3 APR 2025
Accepted 15 JUN 2025

**Author Contributions:**
**Conceptualization:** Jiajian Qiu, Saiyu Yuan
**Funding acquisition:** Saiyu Yuan, Hongwu Tang
**Investigation:** Jiajian Qiu, Yilin Deng
**Methodology:** Jiajian Qiu, Saiyu Yuan
**Project administration:** Hongwu Tang
**Supervision:** Saiyu Yuan, Hongwu Tang
**Writing – original draft:** Jiajian Qiu, Yilin Deng
**Writing – review & editing:** Jiajian Qiu, Saiyu Yuan, Carlo Gualtieri

## Abstract

Large rivers exhibit dynamic and complex geomorphic features, supporting some of the most biodiverse and ecologically productive ecosystems. However, their aquatic ecology is increasingly threatened by human modifications to natural channel morphology. The lack of systematic investigation and understanding of the interactions between hydrodynamics, water quality, and aquatic ecology within large-scale, morphologically complex rivers has led to fragmented ecological management. This study investigates the large-scale responses of fish communities to complex channel morphologies through two comprehensive field surveys of hydrodynamics, water quality, and fish distribution along a ~30 km reach of the Yangtze River, encompassing channel narrowing, bifurcation, and the Yangtze River-Poyang Lake cascading confluence system. Both surveys observed elevated fish densities at the confluence and narrowing section, particularly with a distinct Confluence Hydro-Ecological Zone (CHEZ) within the post-confluence channel, marked by a pronounced increase in fish density and species diversity relative to both upstream and downstream sections. Mixing dynamics driven by the confluence momentum ratio ($M_r$) regulate the CHEZ: slow mixing in the equivalent momentum regime ($M_r \approx 1$) amplified the increase in fish density within the CHEZ, while rapid mixing in the unequal momentum regime ($M_r >> 1$) weakened such effect but expanded the CHEZ. Density of large fish was primarily influenced by water depth and water-quality variability, whereas density of small fish was driven by seasonal population dynamics and hydrodynamic conditions. This study highlights that a comprehensive understanding of hydrodynamic configurations, water-quality contrasts, and seasonal biological dynamics at confluences can inform process-based strategies for sustainable river management.

## Plain Language Summary

Large rivers, like the Yangtze River, support diverse and productive ecosystems, but human modifications to their natural morphology and flow conditions have increasingly threatened aquatic life. One major challenge in ecological conservation is the lack of understanding about how aquatic communities respond to these changes in large, complex river systems. To address this, two field surveys along a more than 30 km stretch of the Yangtze River were conducted to investigate hydrodynamics, water quality, and fish community across different channel features, such as confluences, narrow reaches, and bifurcations. Among these, confluences were observed to have the strongest influence on increased fish density and species numbers. The magnitude and extent of this increase was related to the momentum contrast and mixing processes of the two converging rivers. These findings suggest that adjusting water flow at key locations in large rivers could more effectively sustain fish communities. Understanding these ecological patterns can support better river management and conservation efforts.

## 1. Introduction

Large rivers span vast spatial scales across multiple regional landscapes, exhibiting dynamic and continuous variations in channel morphology from headwaters to estuaries, including meandering, narrowing, bifurcations, and confluences (Vannote et al., 1980). These morphological features govern complex hydrodynamic processes (Best, 1987; Rhoads & Johnson, 2018), sediment erosion and deposition (Riley & Rhoads, 2012), and material transport and mixing (Xu et al., 2022; Yuan et al., 2024), thereby shaping aquatic habitats heterogeneity and exerting profound influences on the structure and function of aquatic biological communities (Boddy et al., 2019; Yuan et al., 2023). For instance, river meandering enhances lateral connectivity and generates distinct velocity gradients and secondary circulations that drive ecological niche differentiation within fish communities (Nagayama & Nakamura, 2018), with rheophilic species aggregating in high-velocity zones along outer banks and lentic species inhabiting low-velocity zones along inner banks. In the lower Mississippi River, channel narrowing induced by flood control levees intensifies localized flow shear forces, scouring deep pools that offer refugia for benthic fish species such as *Polyodon spathula* during low-water conditions, whereas the rigid structural constraints of the levees disrupt river-floodplain hydrological connectivity, leading to the decline of fish populations reliant on floodplain spawning (Fry, 2002). The braided river segments of the Yarlung Tsangpo River create habitat mosaics through the alternating distribution of sandbars and backwater areas, where substrate heterogeneity and organic matter retention sustain high invertebrate diversity (Zhou et al., 2022). At the confluence of the Amazon and Negro rivers, flow shear and mixing processes establishes gradients in turbidity, temperature, and nutrient concentrations, fostering unique planktonic communities and attracting fish aggregations (Gualtieri et al., 2019; Nakajima et al., 2017). Overall, the morphological complexity of large rivers regulates multidimensional hydrodynamic-habitat gradients (Polvi et al., 2020), including velocity stratification, substrate heterogeneity, and material mixing interfaces, which collectively drive the evolutionary processes and adaptive strategies of aquatic biological communities, ultimately supporting some of the richest global biodiversity (Belletti et al., 2020).

Hydrodynamics constitute a fundamental regulatory force governing the spatiotemporal distribution patterns of aquatic communities (Abrial et al., 2019; Qiu et al., 2024; Rhoads et al., 2003). As critical nodes within large river systems, river confluences integrate some of the most complex and diverse hydrodynamic processes (Constantinescu & Gualtieri, 2024; Yuan et al., 2022). The Confluence Hydrodynamic Zone (CHZ), which encompasses the most distinctive set of hydrodynamic features introduced by tributary inflows (Kenworthy & Rhoads, 1995), is characterized by highly intricate three-dimensional flow structures (Constantinescu et al., 2011; Yuan et al., 2021). Such complex flow structures strongly influence the mixing dynamics between converging flows, governing the distance over which complete transverse mixing occurs between the mainstream and tributaries. This process often results in highly variable length scales, typically ranging from a few kilometers to several hundred kilometers (Lane et al., 2008; Meem et al., 2025; Pouchoulin et al., 2020). These interactions contribute to the development of distinctive ecological patterns with large spectrum of habitat complexity around the confluence area (Rice et al., 2006). For highly dispersive aquatic communities such as fish, any increase in habitat heterogeneity is expected to enhance community productivity (Benda et al., 2004), with exceptionally high fish productivity and diversity consistently observed at large confluences across major river basins worldwide, including the Amazon, Mississippi, and Yangtze Rivers (Dettmers et al., 2001; Fernandes et al., 2004; Yuan et al., 2023). While the ecological significance of confluences in large river basins has been widely acknowledged, existing researches predominantly characterized them as biodiversity hotspots in a phenomenological manner, lacking mechanistic insights into the intensity and spatial scale of these ecological effects driven by the unique hydrodynamic processes at river confluences (e.g., Czegledi et al., 2016).

Moreover, globally pervasive anthropogenic activities, including land use modification, river channelization, dam construction, and water diversion/abstraction, have increasingly disrupted the coupling mechanisms between natural morphological features and hydrological processes, thereby leading to habitat homogenization and the decline of fish species diversity (Dudgeon et al., 2006). Therefore, a thorough understanding of how fish communities respond to the diverse hydrodynamic processes driven by river channel morphology is fundamental to predicting river ecosystem evolution and developing targeted conservation strategies. Although previous research has advanced insights into hydrodynamic-biological linkages at localized spatial scales for individual river channel morphologies, such as confluences and meandering reaches (Wang et al., 2025; Yuan et al., 2023), a comprehensive investigation and understanding of fish community response mechanisms to the interplay of spatially varying channel-morphological conditions and spatially heterogeneous hydrodynamic processes at broader spatial scales remains lacking. This limitation primarily stems from the inherent complexity of flow dynamics and logistical challenges associated with large-scale field surveys, including the requirements for specialized instrumentation, labor, and resources. Such a knowledge gap not only restricts the precision of river ecosystem integrity assessments but also leads to fragmented ecological management and conservation by overlooking the longitudinal connectivity of morphological features, potentially enhancing local biodiversity while undermining functional connectivity at the watershed scale.

To this end, this study presents findings from two large-scale comprehensive field surveys along a more than 30 km reach of the Yangtze River, characterized by complex channel morphologies, including narrowing, bifurcation, and a cascading confluence system of the Yangtze River and Poyang Lake. The surveys integrated high-resolution hydrodynamic and ecological assessments using acoustic Doppler velocity profiling, multiparameter water quality measurements, non-invasive hydroacoustic detection of fish density distribution, and environmental DNA assessments for fish species composition to systematically investigate hydrodynamic processes, water quality conditions, and the spatial distribution patterns of fish communities. As the largest river and largest freshwater lake in China, respectively, the Yangtze River and Poyang Lake have a quite large difference in hydrodynamics and water quality during the hydrological cycle, creating highly dynamic spatiotemporal habitat for fish communities at their confluence. This study aims at clarifying the interplay between main habitat drivers (morphology, hydrodynamics, and water quality) and the fish assemblage structure within a large-scale, morphologically complex river reach, with a particular focus on whether the intricate hydrodynamic processes and mixing dynamics within the cascading confluence system generates more pronounced ecological benefits for fish communities. The findings of this study provide a scientific foundation for optimizing hydrodynamic regulation strategies at river confluences, enhancing regional fish community productivity, and advancing systematic ecological conservation and sustainable management of large river basins.

## 2. Materials and Methods

### 2.1. Study Area

The study area is centered on the confluence between the Yangtze River and Poyang Lake, located approximately 900 km downstream of the Three Gorges Dam and 800 km upstream from the Yangtze River estuary (Figure 1a), marking the boundary between the middle and lower reaches of the Yangtze River. Near the Jiujiang Hydrological Station (29.77°N, 116.06°E), the Yangtze River is divided by Zhangjia Island into two branches. The right branch directly converges with the outflow from Poyang Lake at Hukou (29.75°N, 116.21°E), creating the first confluence (CONF1) at an angle of about 58° (Figure 1b). Approximately 6 km further downstream, the converging flow rejoins with the other branch of the Yangtze River with an angle close to 90°, forming the second confluence (CONF2). This study area encompasses the cascading confluence system formed by these two confluences, that is the two reaches of the Yangtze River upstream of the confluences (hereafter referred to as YR1 and YR2; see Figure 1b), the downstream end of the Poyang Lake outflow channel (PL), the channel between the confluences (CC), and a river reach extending 24 km downstream from the second confluence (DS), which encompasses channel bifurcation and narrowing. To further illustrate the spatial variations of fish communities downstream of river confluences subjected to a complex mixing dynamic, the two post-confluence channels, CC and DS, were further segmented. Channel CC, characterized by complex confluence-driven flow structures, was subdivided into three reaches—C1, C2, and C3—each approximately 2 km long (Figure 1c). Channel DS with relatively stable flow structures was classified into a total of eight reaches, numbered D1 to D8, with each reach about 3 km long. This segmentation was based on hydrodynamic observations and aimed to ensure spatial scale comparability across reaches, enabling consistent analysis of ecological and hydrodynamic patterns at a unified resolution.

Two field surveys aimed at measuring multiple hydrodynamics, water quality, and ecological parameters were conducted around the confluence area in April and July 2023. These times of the year hold crucial significance for river-lake fish communities, particularly regarding the population dynamics of potamodromous species, such as black carp, grass carp, silver carp, and bighead carp, which rank among the most economically important fishes in China (Song et al., 2018). In April, as flow discharge and water temperature gradually increase, phytoplankton in the water rapidly proliferates, prompting fish to actively forage in preparation for subsequent spawning. During this period, migratory parent fish pass through the confluence area toward upstream spawning grounds in the Yangtze River (Liu et al., 2019). In the following months, a substantial number of fish eggs continue to drift downstream, and newly hatched juvenile fish seize the opportunity to enter Poyang Lake for feeding and growth, with July marking the peak period for juveniles entering the lake (Hu et al., 2011). Between the two surveys, the discharge at the Jiujiang Hydrological Station (including both branches of the Yangtze River) increased from 14,000 to 26,000 $m^3$/s, while the outflow from Poyang Lake remained around 7,000 $m^3$/s according to the Hukou Hydrological Station (Table 1). Consequently, at the first confluence, the discharge ratio between the Yangtze River and Poyang Lake increased from approximately 1 in April to around 1.8 in July. These differences in discharge ratio and the contrasting water quality properties of these two inflows create distinct mixing dynamics in the post-confluence channel (Xu et al., 2022), offering an ideal scenario for investigating the drivers of fish community productivity downstream of river confluence.

10.1029/2025WR040690

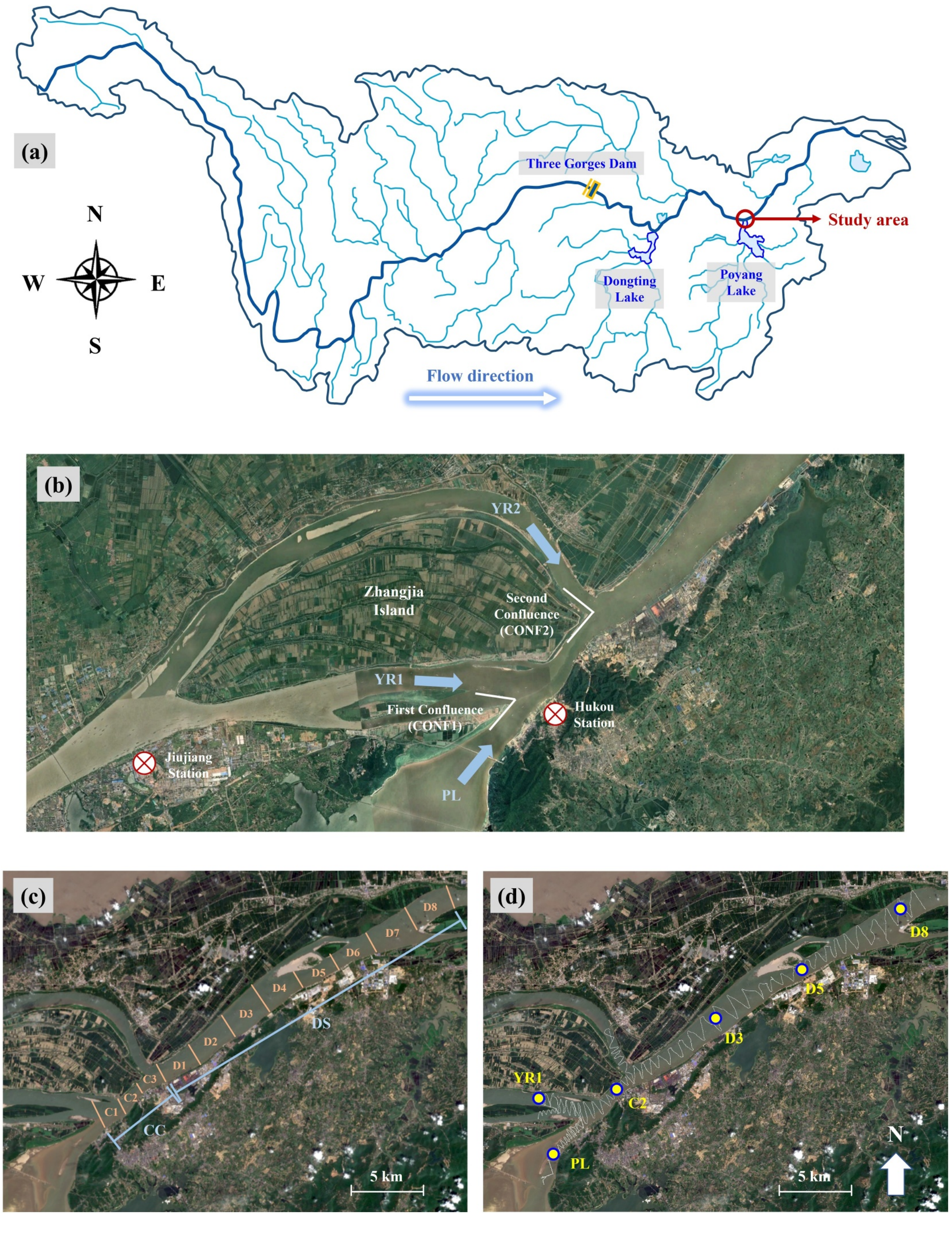


**Figure 1.** (a) Map of the Yangtze River Basin indicating the confluence between the Yangtze River and Poyang Lake, located in the middle to lower reaches of the Yangtze River (29.75°N, 116.21°E). (b) The study area includes two confluences formed by the two branches of the Yangtze River (YR1 and YR2) and the Poyang Lake outflow channel (PL). (c) Two post-confluence channels (CC and DS), which are further subdivided into several reaches for detailed analysis. (d) The white lines mark the survey trajectory for physical habitat measurements and fish hydroacoustic detection, while the yellow circular symbols represent environmental DNA sampling sites.

### 2.2. Field Surveys

The field surveys were carried out around the confluence area to assess spatiotemporal distribution of hydrodynamic parameters (water depth $H$ and depth-averaged flow velocity $U$) and water quality parameters (conductivity $C$, water temperature $T$, dissolved oxygen content $DO$, chlorophyll a level $Chl$, and turbidity $Turb$). To

**Table 1**
*Main Hydraulic Parameters at the Confluence of the Yangtze River and the Poyang Lake*

| Hydraulic parameters | | April survey | July survey |
|---|---|---|---|
| Water level (m) | YR1 | 11.24 | 14.86 |
| | PL | 11.34 | 14.99 |
| Discharge $Q$ (m3/s) | YR1 | 7,450 | 13250 |
| | PL | 7,350 | 7,280 |
| Discharge ratio $Qr$ | | 1 | 1.8 |
| Flow velocity $U$ (m/s) | YR1 | 0.74 | 0.92 |
| | PL | 0.72 | 0.47 |
| Velocity ratio $Ur$ | | 1 | 2 |
| Momentum ratio $Mr$ | | 1 | 3.6 |
| Channel width $W$ (km) | YR1 | 1.3 | 1.5 |
| | PL | 0.9 | 0.9 |
| | CC | 2.2 | 2.3 |
| Mixing length $L$ (km) | | >30 | 12 |
| $L$:$WCC$ | | >14 | ~5 |

*Note.* The water levels of YR1 and PL are derived from the records of the Jiujiang and Hukou Hydrological Stations, respectively. The discharge of YR1 is assumed to be half of the recorded discharge at the Jiujiang Hydrological Station, whereas the discharge of PL corresponds to the recorded discharge at the Hukou Hydrological Station. The flow velocity $U$ is average value of the depth-averaged flow velocity measured with ADCP. $Q_r = \frac{Q_{YR1}}{Q_{PL}}$, $U_r = \frac{U_{YR1}}{U_{PL}}$, $M_r = \frac{\rho_{YR1}}{\rho_{PL}} Q_r U_r$, assuming $\rho_{YR1} \approx \rho_{PL}$, where $\rho$ indicates fluid density.

continuously monitor hydrodynamic and near-surface water quality parameters over a large-scale area, a Sontek River Surveyor M9 acoustic Doppler current profiler (ADCP) and a YSI EXO2 multi-parameter probe (YSI) were mounted on a survey vessel, which followed a pre-designed navigation trajectory (Figure 1d). The real-time position of the survey vessel was provided by the differential global positioning system (DGPS) built into the ADCP, offering centimeter-range accuracy. Sensors of these two instruments were tested prior to each measurement according to the manufacturer specification and were fixed at 0.5 m below the water surface, orienting vertically downward during the survey. More details of the on-site configurations and field procedures have been described in Yuan et al. (2021) and Xu et al. (2022).

The spatiotemporal distribution of fish density within the confluence area was characterized by fish hydroacoustic detection, using a BioSonics DT-X split-beam echosounder (DT-X) with a 200 kHz transducer and 7° beam width. This instrument was deployed alongside the ADCP and YSI, with its transducer fixed at the same depth and aimed vertically downward, enabling synchronized measurements of fish density distribution and physical habitat parameters. During the surveys, fish body length information was inferred from the Target Strength (TS), which reflects the echo intensity of individual fish as recorded by the DT-X (Egerton et al., 2021). By applying different filtering thresholds, distribution patterns of fish in various size classes were identified. According to the classification by Bean et al. (1996), the detected fish were grouped into small-, medium-, and large-sized, corresponding to body lengths of 2–20 cm (i.e., $-60$ dB $<$ TS $<$ $-40$ dB), 20–60 cm ($-40$ dB $<$ TS $<$ $-30$ dB), and longer than 60 cm (TS $>$ $-30$ dB), respectively. The DT-X acoustic data were processed with BioSonics Visual Analyzer software 4.1, where specific filtering thresholds were set to distinguish fish across size classes, and fish density distribution was determined through echo integration. Further details on field operation procedures and software applications can be found in Yuan et al. (2023) and Qiu et al. (2024).

Environmental DNA provides additional information on fish species composition that cannot be identified through hydroacoustic detection alone (Hanfling et al., 2016). Due to constraints in field sampling conditions, environmental DNA sampling was only conducted during the April survey. Six sampling sites were strategically positioned around the confluence area, including one point each within the upstream mainstream channel YR1 and tributary channel PL, as well as within post-confluence channel reaches C2, D3, D5, and D8 (Figure 1d). Each sampling site was maintained over 5 km from one another to effectively minimize the potential contamination from upstream DNA fragments. Three sets of three parallel 1-L samples were collected at each sampling site from the surface, middle, and bottom layers, respectively, to ensure a comprehensive representation of the local fish species composition. The collected water samples were filtered, extracted, amplified, and sequenced within 48 hr, following the specific procedures outlined by Yuan et al. (2023). Fish species composition identified through environmental DNA was recorded as presence-absence data for each species.

### 2.3. Data Post-Processing

To clearly present the spatial variations in channel-morphological and hydraulic characteristics downstream of the confluence, the water depth and depth-averaged flow velocity along the survey trajectory were interpolated onto rectangular grids covering the entire study area using a Kriging interpolation procedure. This method provides a highly accurate linear unbiased estimation and is widely applied in geostatistics (Herrero et al., 2018). Within each delineated channel reach downstream of the confluences (i.e., C1–C3 and D1–D8), statistical summaries were compiled for each water quality parameter, including the maximum, minimum, mean, and upper and lower quartile. Conductivity was used as an indicator of the water quality properties of the two merging flows, with its values interpolated across the study area using the same interpolation method as for the hydraulic parameters, to capture the mixing processes downstream of the confluences.

The Inverse Distance Weighting (IDW) interpolation method was applied to map the fish density data collected by the DT-X onto grids across the study area. By assigning greater weight to nearby data points, this method is particularly effective at capturing local spatial variation in fish density, which is a valuable feature in highly dynamic aquatic environments (Coley & Clabburn, 2005). To quantify the impact of the confluence on fish density, change from upstream to downstream in the average fish density was estimated, that is, from YR1 and PL to CC, and from CC and YR2 to DS. For DS, only reaches D1 and D2 were included to maintain a channel length comparable to CC. The change in fish density is defined as:

$$\Delta = \frac{\mathrm{FD}_{\mathrm{post}} - \mathrm{FD}_{\mathrm{pre}}}{\mathrm{FD}_{\mathrm{pre}}} \times 100\%$$

where $\mathrm{FD}_{\mathrm{pre}}$ is the average fish density on the higher-density side of the two pre-confluence tributaries, $\mathrm{FD}_{\mathrm{post}}$ is the fish density in the post-confluence channel, and $\Delta$ quantifies the variation in fish density in the post-confluence channel relative to the higher-density pre-confluence tributary. The average fish density for each reach within the post-confluence channels, specifically C1 to C3 and D1 to D8, was calculated to reflect the longitudinal distribution of the fish assemblage downstream of the two confluences.

Based on the fish species composition identified with environmental DNA at different sampling sites, K-means clustering analysis (*R* package "stats," function "kmeans") was applied to delineate distinct clusters within the confluence area, clarifying the effects of river confluence on the fish species distributions across upstream and downstream channels. The optimal cluster number $K$ was selected using the elbow method, where $K = 3$ was chosen to balance minimized within-cluster variance and avoid overfitting.

To identify the driving effects of spatiotemporal variations in downstream habitats on fish community, a redundancy analysis (RDA; *R* package "vegan," function "ca") was used to relate fish assemblage data and habitat characteristics. Fish densities across small, medium, and large size classes, derived from hydroacoustic detection, served as indicators of fish community productivity for the analysis. Habitat parameters included two hydrodynamic parameters measured by ADCP, five water quality parameters measured by YSI, as well as their respective variation ranges, defined as the difference between the maximum and minimum values within each channel reach. Parameters with significant effects on fish density, as determined by permutation tests, were retained for the analysis.

## 3. Results

### 3.1. Distribution Patterns of Habitat Parameters at the Confluence

Routine measurements from Jiujiang and Hukou hydrological stations indicate that the water levels in channels YR1 and PL were closely aligned. Between the April and July surveys, the water level in both channels increased by about 3.6 m (Table 1). The increase in water level within channel YR1 resulted in an expansion of its width from 1.3 to 1.5 km, while the width of channel PL remained largely stable at approximately 0.9 km. Between the two surveys, the width of channel CC, the post-confluence channel between YR1 and PL, ranged from 2.2 to 2.3 km. A deep scour hole with a water depth exceeding 16 m was observed in channel CC during both surveys, extending downstream to the end of channel DS (Figure 2). The channel morphology downstream of CONF1 responded to changes in upstream flow conditions. During the April survey, the discharges in channels YR1 and PL were approximately equivalent, with a small momentum ratio $M_r$ close to 1, resulting in a minimal backwater effect from the Yangtze River to the Poyang Lake. A high-velocity outflow was observed within channel PL, with an average velocity of approximately 0.7 m/s and a maximum velocity exceeding 1 m/s (Table 1 & Figure 3), comparable to those in channel YR1. In contrast, during the July survey, the discharge of YR1 was nearly twice that of PL, with YR1 maintaining a generally high velocity close to 1 m/s. The outflow from Poyang Lake was increasingly impeded by the Yangtze River, dropping the average outflow velocity in channel PL to about 0.5 m/s. The momentum ratio $M_r$ increased dramatically to 3.6. The increased incoming discharge in July extended the high-velocity area in the post-confluence channels, leading to a scour hole wider than that observed in April. Notably, near the apex of CONF2, where YR2 merges with CC, the additional flow created a high-velocity area that scoured out a large, deep pit exceeding 30 m in depth. Additionally, the river bifurcates at reach D5, with the channel narrowing inducing localized high-velocity conditions, leading to extensively scouring there.

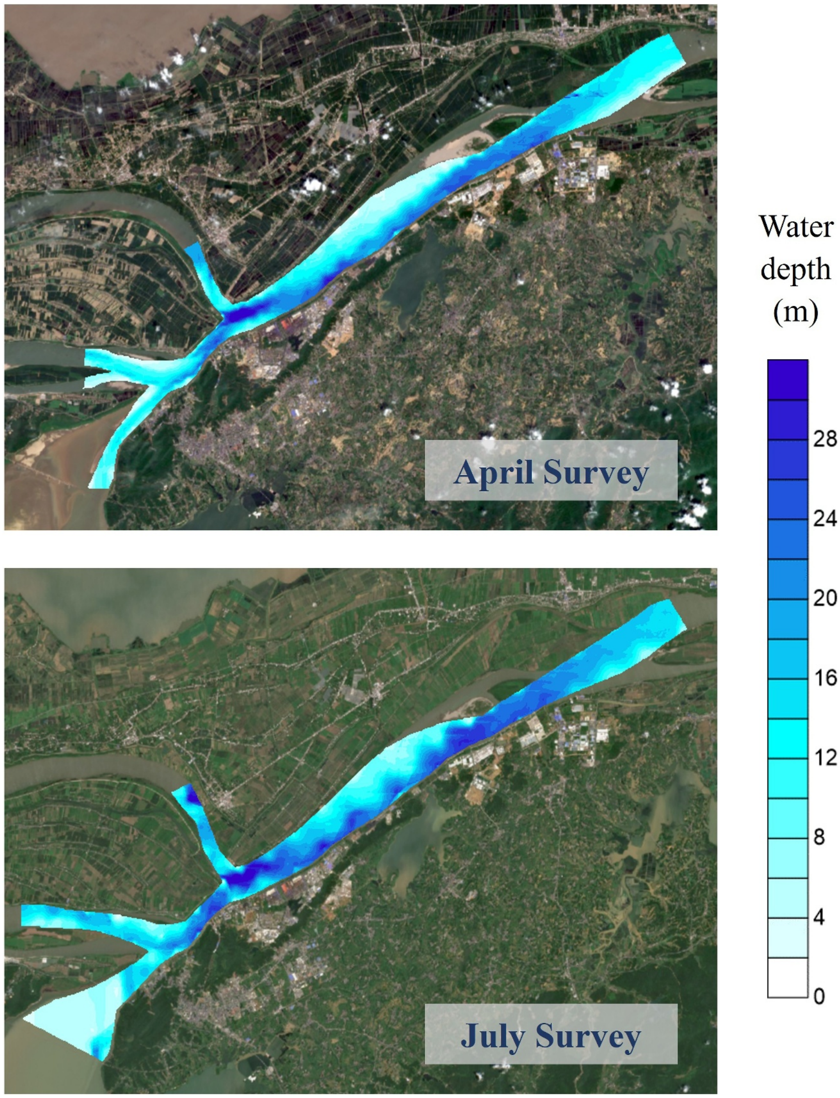


**Figure 2.** Bathymetry of the study area during the field surveys.

The inflows from the Yangtze River and Poyang Lake, each characterized by distinct water quality properties, underwent extensive mixing within the confluence area. The initial confluence reach C1 had the widest range of hydrodynamics and water quality conditions (Figure 4). As the mixing between the two converging flows progressed, the spatial heterogeneity of water quality parameters gradually decreased downstream. At CONF2, the inflow from channel YR2, another branch of the Yangtze River, created a transition point in reach D1 that disrupted the previously longitudinal trend of water quality variation. However, while the tributary input introduced additional water quality complexity at CONF1, the inflow from channel YR2 instead constrained the variability of water quality parameters, a phenomenon particularly pronounced in the July survey. This effect can be attributed to the high similarity in water quality properties between flows from channels YR2 and YR1, both originating from the Yangtze River. The channel YR2 inflow diluted the relative contribution of Poyang Lake outflow, accelerating the stabilization of downstream water quality conditions toward a state closely resembling the pre-confluence properties of the Yangtze River.

During the April survey, the mixing interface between the two inflows in C1 was particularly narrow, with the lateral distribution of near-surface conductivity displaying a more abrupt transition between the two flows compared to the July survey (Figure 5). Downstream, the mixing process gradually developed, leading to a progressive narrowing of the variation range in water quality parameters. During the July survey, the mixing

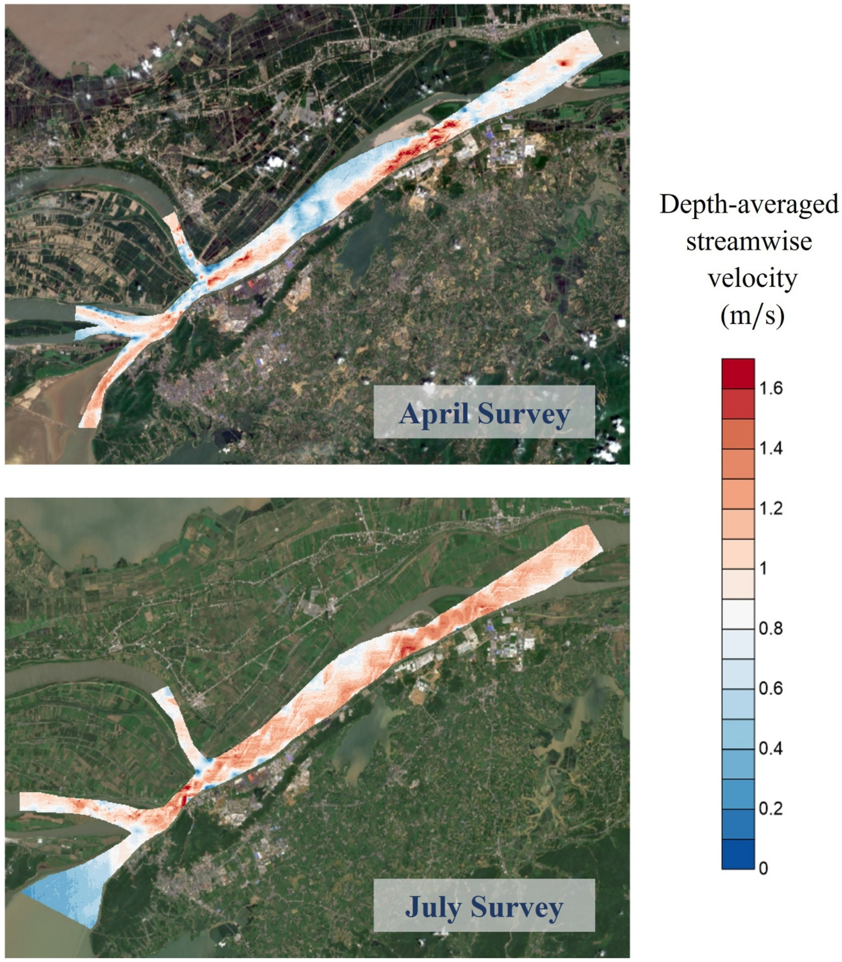


**Figure 3.** Map of the depth-averaged streamwise velocity in the study area during the field surveys.

process was notably rapid, with the flows in the vicinity of D2 essentially achieving complete mixing. The mixing length, here defined as the distance from the confluence apex of CONF1 to the location where complete mixing occurs, was approximately 9 km, equivalent to five times the width of post-confluence channel CC (Table 1). In contrast, during the April survey, the mixing of the two flows was considerably slower, reaching a near-complete state only near D8. The mixing length in this case exceeded 30 km and corresponded to more than 14 times the width of channel CC. It is noteworthy that, during the July survey, the lower-conductivity flow from Poyang Lake traversed over the higher-conductivity flow from Yangtze River within C3 and D1, positioning itself on the left side of the channel. This arrangement produced a lateral distribution pattern of near-surface conductivity that was opposite to that observed upstream. In contrast to the distinct segregation of the Yangtze River and Poyang Lake flows in the April survey, where each flow was clearly positioned on opposite sides of the post-confluence channel, this transposed mixing structure facilitated faster mixing between the two converging flows, explaining the accelerated mixing process observed in the July survey.

### 3.2. Spatiotemporal Heterogeneity of Fish Assemblage at the Confluence

Large spatiotemporal heterogeneity in fish density was found within the confluence area, upstream and downstream of the junction (Figure 6). At CONF1, the average fish density across all size classes within the post-confluence channel CC increased greatly relative to those in the upstream mainstream and tributary during both surveys. The largest increase in fish density, reaching 150%, was observed in medium-sized fish during the April survey, while the smallest increase, about 30%, was recorded for small-sized fish during the same period. This enhancement effect of river confluence on fish density made the first post-confluence channel CC a density hotspot, supporting the highest observed fish densities across all size classes in both surveys. At CONF2, the

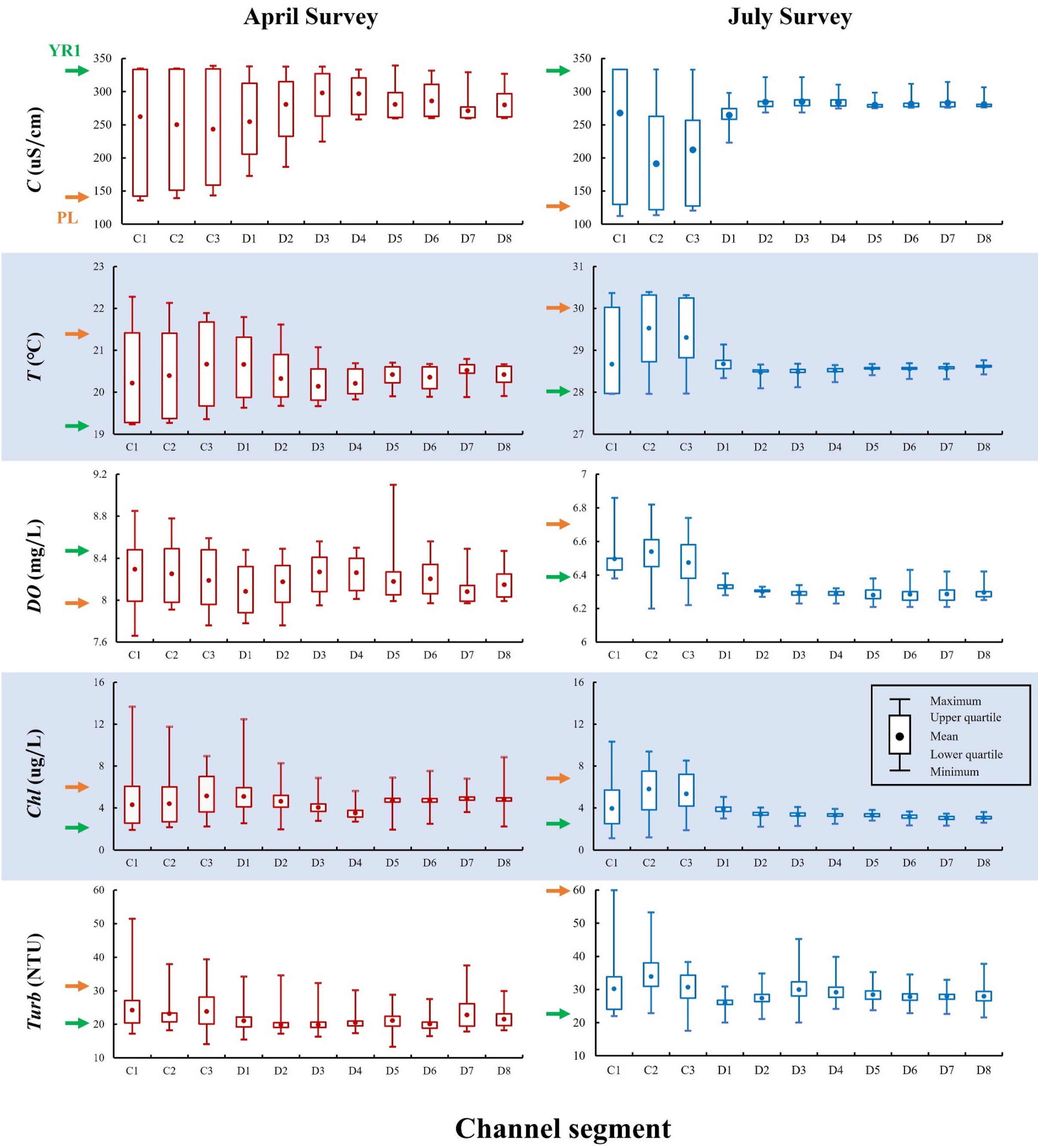


**Figure 4.** Spatiotemporal variations in near-surface water quality parameters downstream of the confluences between the Yangtze River and Poyang Lake (CONF1 and CONF2). Statistical values, including the maximum, minimum, mean, and upper and lower quartile for each water quality parameter, were summarized. Water quality parameters include conductivity (*C*), water temperature (*T*), dissolved oxygen concentration (*DO*), chlorophyll a level (*Chl*), and turbidity (*Turb*). The green and orange arrows indicate the pre-confluence mean values of each water quality parameter within the Yangtze River channel (YR1) and the Poyang Lake channel (PL), respectively.

expected enhancement effect on fish density was no longer observed. This may be attributed to the already elevated fish density in the tributary channel CC, as well as to the relatively minor differences in water quality between the converging flows at this junction, which was unable to provide additional habitat heterogeneity for fish communities compared to the CONF1. Apparently, a cascade of confluences over short spatial scales, particularly those involving tributaries with similar water quality properties, does not contribute to a cumulative increase in fish density.

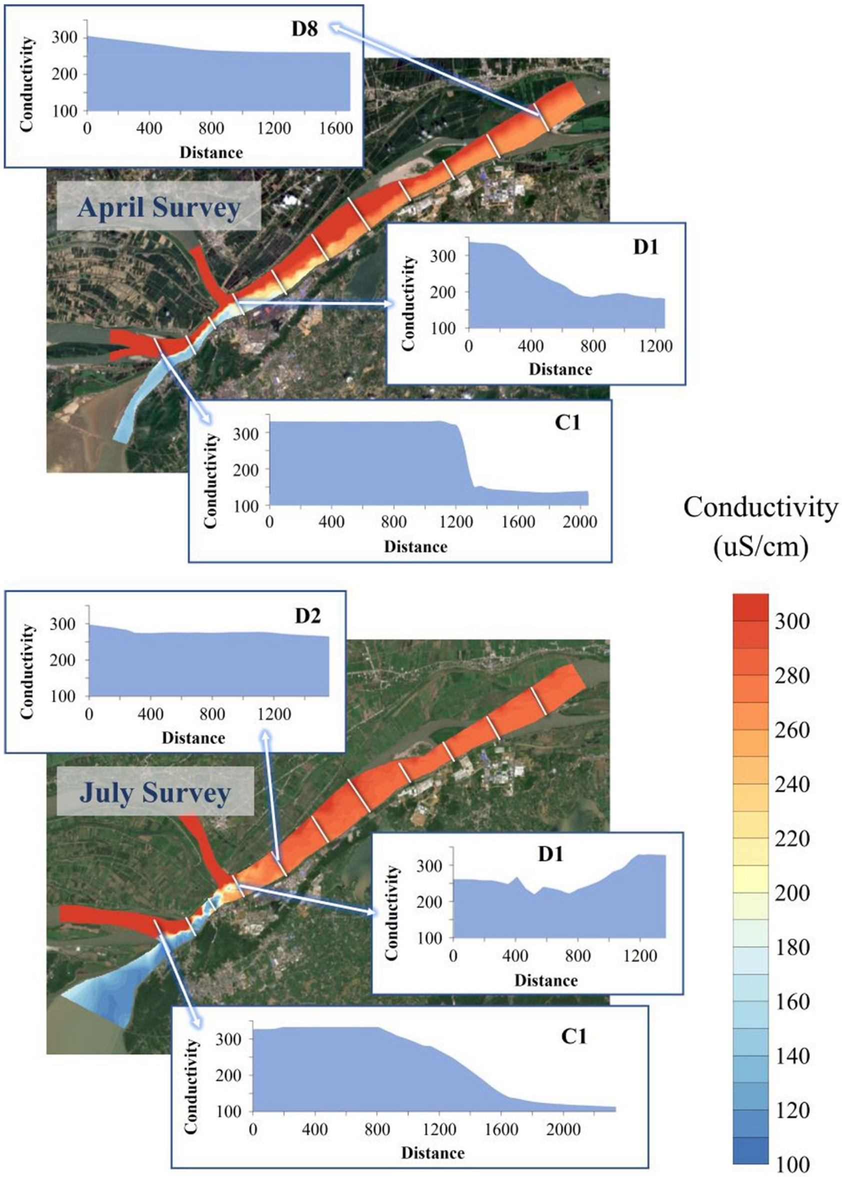


**Figure 5.** Map of near-surface conductivity distribution in the study area during the field surveys. Lateral distribution of conductivity at several key cross-sections indicates the dynamic mixing processes downstream of the confluences.

Fish density longitudinally fluctuated along the post-confluence channel (Figure 7), with one peak occurring between reaches C2 and C3, another in D5, and a low point in D3. The first peak points out the confluence-induced effect on fish density, limited to a localized area immediately downstream of the junction. The area presenting such an enhancement effect driven by confluence hydrodynamics was herein defined as the Confluence Hydro-Ecological Zone (CHEZ), specifically referring to the region of the confluence where the average fish density exceeds that upstream in the mainstream and tributary. Reach C1, despite fish density being generally lower than that in the pre-confluence channel YR1, was still classified within the CHEZ due to its typical hydraulic characteristics associated with the confluence dynamics. During the July survey, the CHEZ for all fish size classes extended from the initial confluence reach to D2. Its spatial extent reached five times the width of post-confluence channel CC, comparable to the mixing length observed in July. In contrast, during the April survey, the spatial extent of the CHEZ varied slightly among fish size classes but remained consistently more limited than in July, extending at most to reach D1, with a length lower than four times the width of channel CC. The second peak in fish density was primarily driven by morphological changes in the straightened channel, as the channel

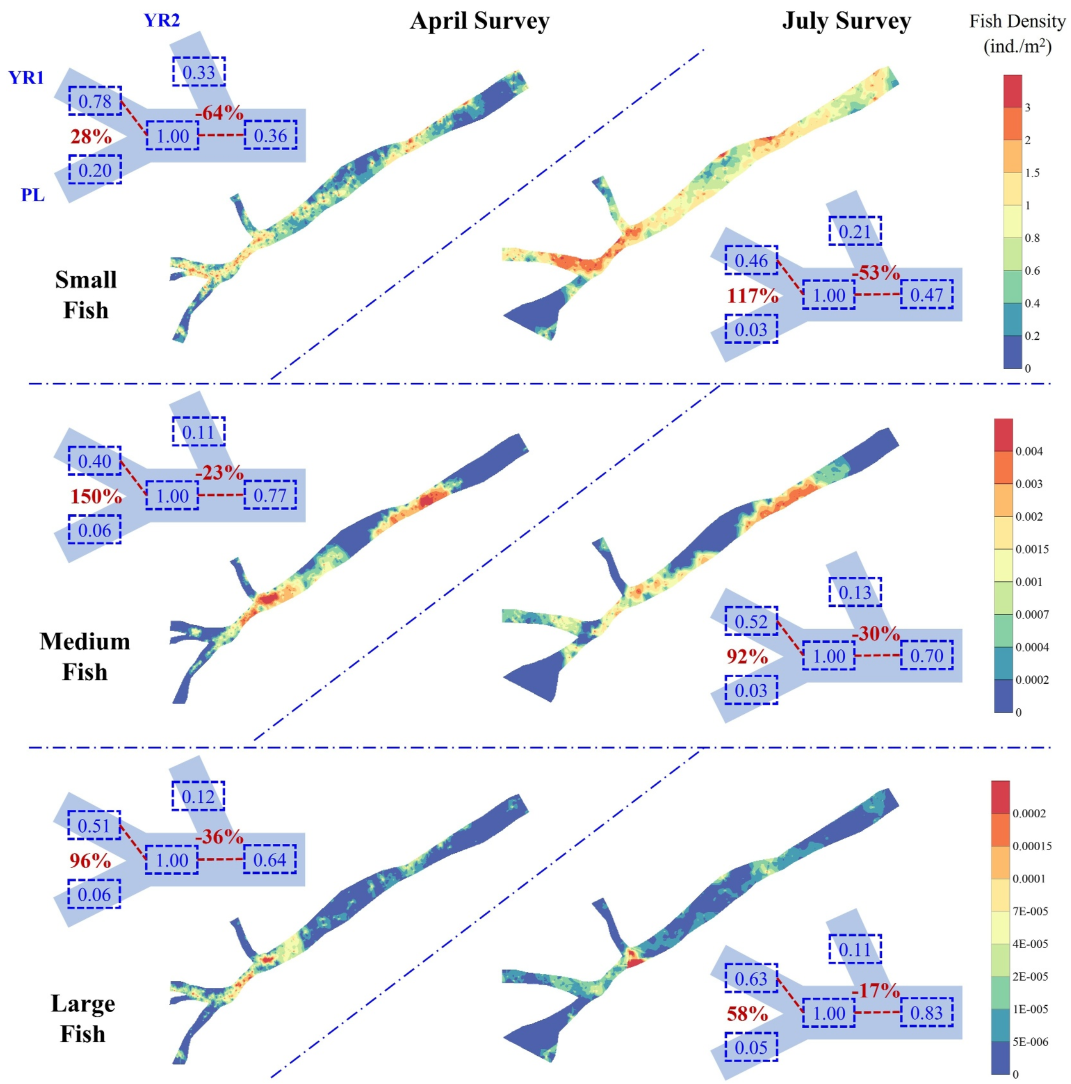


**Figure 6.** Map of fish density distribution for small-, medium-, and large-sized classes in the study area during the field surveys. The simplified river channel diagrams mark the min-max normalized average fish density across five channels (i.e., YR1, PL, CC, YR2, and DS), as well as indicate the variation in fish density in the post-confluence channel relative to the higher-density pre-confluence tributary, generally from YR1 to CC and from CC to DS.

bifurcation and narrowing observed in reach D5 seemed to create favorable habitat conditions, particularly benefiting medium-sized fish. It is apparent that, beyond river confluences, other complex river channel morphologies also have considerable ecological significance for fish communities.

Comparatively, the CHEZ had a stronger density enhancement effect on medium- and large-sized fish during the April survey than during July survey (Figures 6 and 7). In contrast, during the July survey, the density of small-sized fish was much higher in the CHEZ, with the C1 exhibiting over five times the density observed during the April survey. Such considerable increase was likely driven by an influx of juvenile fish from upstream, as July coincides with the peak spawning period in the Yangtze River Basin. Furthermore, the reduced outflow velocity from Poyang Lake may promote aggregation of these juveniles near the confluence apex, providing them with favorable conditions to enter the tributary lake for feeding and growth. Downstream of the CHEZ, fish densities across all size classes observed during the July survey were consistently higher than those observed in April, likely due to the reproductive dynamics inherent to the typical life history of the local fish community. Nevertheless, the longitudinal trends in fish density between the two surveys exhibited striking similarity, suggesting

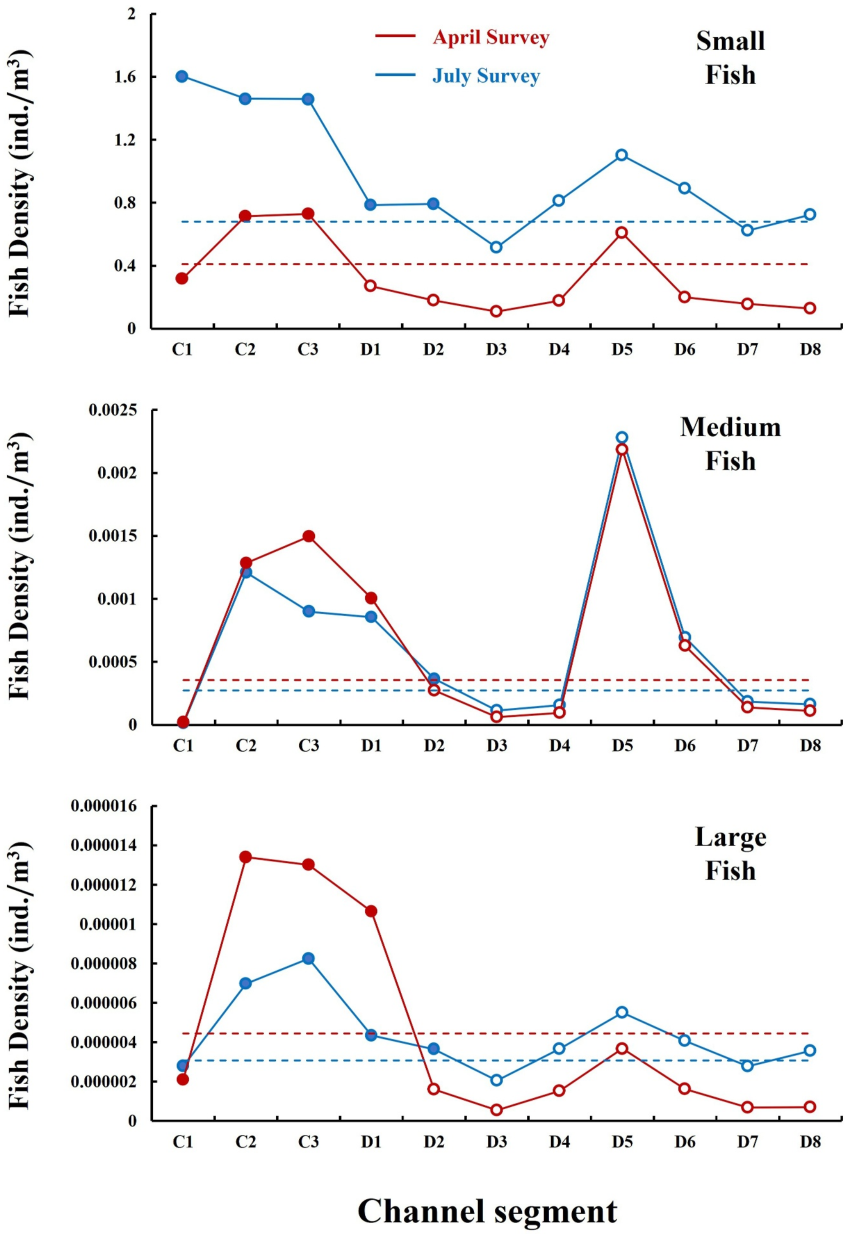


**Figure 7.** Longitudinal distribution of average fish density for small-, medium-, and large-sized classes within each reach along the post-confluence channels. The dashed line denotes average fish density in the pre-confluence channel of the Yangtze River (channel YR1). Solid circles indicate the reaches within the Confluence Hydro-Ecological Zone (CHEZ).

that seasonal variations in hydrodynamic processes and mixing dynamics related to the confluence did not influence fish spatial distribution patterns beyond the CHEZ.

A total of 50 fish species, belonging to 9 families and 4 orders, were identified by environmental DNA around the confluence area during the April survey (Table 2). Among these identified species, Cyprinidae fish within the order Cypriniformes showed the greatest diversity, encompassing 33 species, whereas only a single species was recorded from the order Clupeiformes. The *K*-means clustering analysis categorized all sampling reaches into three distinct clusters (Figure 8), with the mainstream channel YR1 and reaches D2, D5, and D8 downstream of the confluences forming one cluster, while the tributary channel PL and the post-confluence channel reach C2 each constituted separate clusters. The latter two clusters both had the highest species richness, each containing 36 species, of which 27 were found to co-occur in the two reaches. Channel YR1 and reaches D2, D5, and D8

**Table 2**
*Fish Species Composition Identified With Environmental DNA in the Study Area During the Field Surveys*

| Order | Family | Scientific name | Sampling site | | | | | |
|---|---|---|---|---|---|---|---|---|
| | | | YR1 | PL | C2 | D3 | D5 | D8 |
| Clupeiformes | Engraulidae | *Coilia nasus* | 1 | 1 | 1 | 1 | 1 | 1 |
| Cypriniformes | Cobitidae | *Misgurnus anguillicaudatus* | 1 | 1 | 1 | 1 | 1 | 0 |
| Cypriniformes | Cobitidae | *Parabotia fasciata* | 0 | 1 | 0 | 0 | 0 | 0 |
| Cypriniformes | Cyprinidae | *Acheilognathus barbatus* | 1 | 1 | 0 | 0 | 0 | 0 |
| Cypriniformes | Cyprinidae | *Acheilognathus chankaensis* | 1 | 1 | 1 | 1 | 1 | 1 |
| Cypriniformes | Cyprinidae | *Carassius auratus* | 1 | 1 | 1 | 1 | 1 | 1 |
| Cypriniformes | Cyprinidae | *Chanodichthys erythropterus* | 1 | 1 | 1 | 0 | 0 | 0 |
| Cypriniformes | Cyprinidae | *Chanodichthys mongolicus* | 1 | 1 | 1 | 1 | 0 | 1 |
| Cypriniformes | Cyprinidae | *Ctenopharyngodon idella* | 0 | 1 | 1 | 1 | 1 | 1 |
| Cypriniformes | Cyprinidae | *Culter alburnus* | 0 | 1 | 0 | 0 | 0 | 0 |
| Cypriniformes | Cyprinidae | *Cyprinus carpio* | 1 | 1 | 1 | 1 | 1 | 1 |
| Cypriniformes | Cyprinidae | *Distoechodon tumirostris* | 0 | 1 | 1 | 0 | 0 | 0 |
| Cypriniformes | Cyprinidae | *Elopichthys bambusa* | 0 | 0 | 1 | 1 | 1 | 1 |
| Cypriniformes | Cyprinidae | *Gnathopogon polytaenia* | 0 | 0 | 1 | 0 | 0 | 0 |
| Cypriniformes | Cyprinidae | *Hemibarbus maculatus* | 0 | 0 | 1 | 0 | 0 | 0 |
| Cypriniformes | Cyprinidae | *Hemiculter leucisculus* | 1 | 1 | 1 | 1 | 1 | 1 |
| Cypriniformes | Cyprinidae | *Hemiculterella sauvagei* | 0 | 1 | 1 | 1 | 0 | 0 |
| Cypriniformes | Cyprinidae | *Hypophthalmichthys molitrix* | 0 | 0 | 1 | 1 | 1 | 1 |
| Cypriniformes | Cyprinidae | *Hypophthalmichthys nobilis* | 1 | 1 | 1 | 1 | 1 | 1 |
| Cypriniformes | Cyprinidae | *Megalobrama amblycephala* | 0 | 1 | 0 | 0 | 0 | 0 |
| Cypriniformes | Cyprinidae | *Megalobrama skolkovii* | 1 | 1 | 1 | 1 | 1 | 1 |
| Cypriniformes | Cyprinidae | *Megalobrama terminalis* | 0 | 0 | 1 | 0 | 0 | 0 |
| Cypriniformes | Cyprinidae | *Mylopharyngodon piceus* | 0 | 0 | 0 | 0 | 0 | 1 |
| Cypriniformes | Cyprinidae | *Onychostoma macrolepis* | 0 | 1 | 0 | 0 | 0 | 0 |
| Cypriniformes | Cyprinidae | *Opsariichthys uncirostris* | 0 | 1 | 1 | 0 | 0 | 0 |
| Cypriniformes | Cyprinidae | *Pseudobrama simoni* | 1 | 1 | 1 | 1 | 1 | 1 |
| Cypriniformes | Cyprinidae | *Pseudolaubuca sinensis* | 0 | 1 | 0 | 0 | 0 | 0 |
| Cypriniformes | Cyprinidae | *Rhodeus lighti* | 0 | 1 | 0 | 0 | 0 | 0 |
| Cypriniformes | Cyprinidae | *Rhynchocypris lagowskii* | 0 | 0 | 0 | 1 | 0 | 0 |
| Cypriniformes | Cyprinidae | *Sarcocheilichthys nigripinnis* | 1 | 1 | 1 | 1 | 1 | 1 |
| Cypriniformes | Cyprinidae | *Saurogobio dabryi* | 0 | 0 | 1 | 0 | 0 | 0 |
| Cypriniformes | Cyprinidae | *Saurogobio gracilicaudatus* | 0 | 0 | 0 | 0 | 1 | 0 |
| Cypriniformes | Cyprinidae | *Squalidus argentatus* | 0 | 1 | 1 | 0 | 0 | 0 |
| Cypriniformes | Cyprinidae | *Squaliobarbus curriculus* | 0 | 1 | 1 | 0 | 0 | 0 |
| Cypriniformes | Cyprinidae | *Xenocypris argentea* | 0 | 1 | 1 | 0 | 1 | 0 |
| Cypriniformes | Cyprinidae | *Zacco platypus* | 0 | 1 | 1 | 0 | 0 | 0 |
| Perciformes | Channidae | *Channa argus* | 0 | 1 | 1 | 0 | 0 | 1 |
| Perciformes | Cichlidae | *Coptodon zillii* | 1 | 1 | 1 | 0 | 0 | 0 |
| Perciformes | Gobiidae | *Mugilogobius myxodermus* | 0 | 1 | 1 | 0 | 0 | 0 |
| Perciformes | Gobiidae | *Rhinogobius cliffordpopei* | 0 | 1 | 0 | 0 | 0 | 0 |
| Perciformes | Gobiidae | *Rhinogobius giurinus* | 1 | 1 | 1 | 1 | 1 | 1 |
| Perciformes | Mastacembelidae | *Mastacembelus sinensis* | 0 | 0 | 1 | 0 | 0 | 0 |

**Table 2**
*Continued*

| Order | Family | Scientific name | Sampling site YR1 | PL | C2 | D3 | D5 | D8 |
|---|---|---|---|---|---|---|---|---|
| Perciformes | Odontobutidae | *Micropercops swinhonis* | 1 | 1 | 1 | 0 | 0 | 0 |
| Perciformes | Odontobutidae | *Odontobutis potamophila* | 0 | 1 | 0 | 0 | 0 | 0 |
| Perciformes | Serranidae | *Siniperca chuatsi* | 0 | 0 | 0 | 0 | 0 | 1 |
| Perciformes | Serranidae | *Siniperca scherzeri* | 0 | 0 | 1 | 0 | 0 | 0 |
| Siluriformes | Bagridae | *Pseudobagrus tenuis* | 0 | 0 | 0 | 0 | 0 | 1 |
| Siluriformes | Bagridae | *Tachysurus eupogon* | 0 | 0 | 1 | 0 | 0 | 0 |
| Siluriformes | Bagridae | *Tachysurus fulvidraco* | 0 | 1 | 1 | 0 | 0 | 0 |
| Siluriformes | Bagridae | *Tachysurus nitidus* | 1 | 1 | 1 | 1 | 0 | 0 |
| Identified species number | | | **17** | **36** | **36** | **18** | **16** | **18** |

*Note.* The values 0 and 1 represent species absence and presence, respectively, within each corresponding sampled channel reaches.

presented a relatively lower species diversity, ranging from 16 to 18 species. The inflow of a tributary with high species diversity introduced discontinuities in species composition within the upstream mainstream, creating localized hotspots of biodiversity in the CHEZ of post-confluence channel. Moving downstream and further away from the CHEZ, the fish communities reverted to lower species richness comparable to those observed in the mainstream upstream of the junction. Therefore, in terms of species diversity, channel morphologies characterized by bifurcation and narrowing did not exhibit ecological benefits comparable to those observed at confluences.

### 3.3. Driving Effects of Hydrodynamics and Water Quality on Fish Assemblage

The RDA constrained to the hydrodynamics and water quality parameters with significant effects on fish assemblage, identified through permutation tests, within the post-confluence channels during the two surveys is shown in Figure 9. The first two axes explain a total of 68.23% of the variance in fish assemblage traits, indicating an important contribution by the hydrodynamics and water quality parameters to the spatiotemporal density distribution of fish communities downstream of the confluences. A positive correlation between water depth $H$ and the variation ranges of flow velocity $\Delta U$, water temperature $\Delta T$, and conductivity $\Delta C$ was found, with these parameters being effectively represented by the Axis 1 of RDA. This axis reflected the habitat complexity, encompassing both the water depth and the variability of water quality parameters, while it also distinguished between levels of fish community productivity. Except for D5, another segment with complex river morphology, all reaches clustered on the positive side of Axis 1 were situated within the core confluence zone, where intensive mixing processes between the two converging flows were active. This zone closely aligned with the CHEZ, characterized by a pronounced increase in fish densities across all size classes, along with elevated species diversity. In contrast, reaches placed on the negative side of Axis 1 were predominantly located outside the CHEZ, with relatively lower fish densities and species richness. Channel reaches from different surveys were positioned on opposite sides of Axis 2, surveys in July characterized by higher flow velocities and water temperatures grouping on the positive side, whereas in April they were clustered on the other side. Furthermore, the density of small-sized fish responded to the gradient along Axis 2, with the hydrodynamics and water quality conditions in July supporting higher densities of small-sized fish around the confluence area, indicating a more evident seasonal dynamic in their populations compared to other size classes.

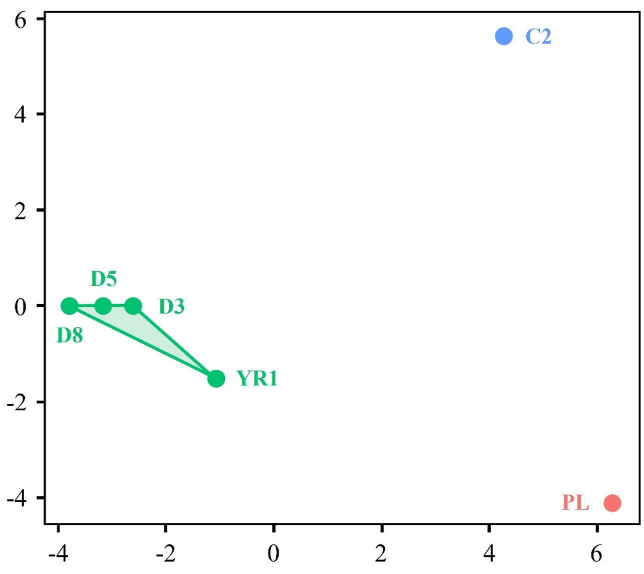


**Figure 8.** K-means cluster analysis for sampled reaches based on fish species composition identified with environmental DNA.

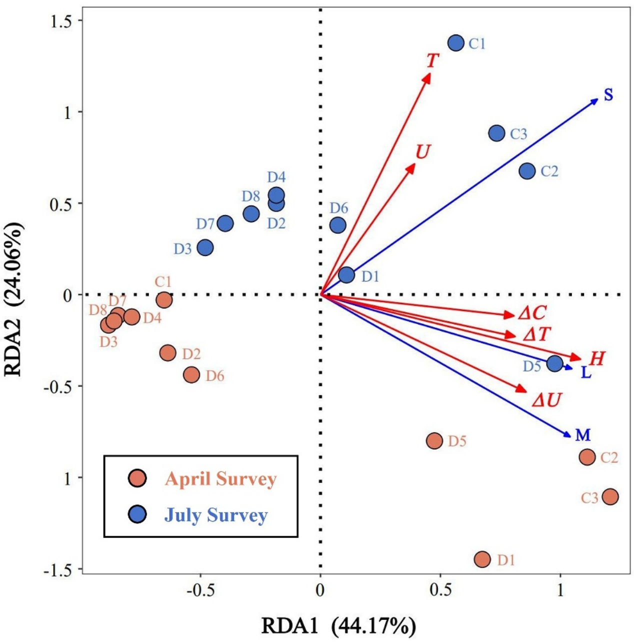


**Figure 9.** Redundancy analysis (RDA) diagram for fish assemblage, as well as hydrodynamics and water quality parameters within the post-confluence channels. Fish densities across small (S), medium (M), and large (L) size classes were included as fish assemblage traits. Hydrodynamics and water quality parameters with significant effects on fish densities identified through permutation tests: water depth ($H$), flow velocity ($U$), variation range of velocity ($\Delta U$), water temperature ($T$), variation range of water temperature ($\Delta T$), and variation range of conductivity ($\Delta C$).

## 4. Discussion

River channel morphology and hydrodynamic processes undergo dynamic co-evolution through persistent interactions and feedback mechanisms, wherein channel morphologies such as meandering, narrowing, bifurcations, and confluences not only emerge as products of sediment transport dynamics but also serve as fundamental drivers of aquatic habitat heterogeneity (Best, 1987; Rice et al., 2006). In the present study, elevated fish densities were observed across river reaches exhibiting various complex morphological characteristics, corroborating previous findings from localized studies focused on individual channel morphologies. For example, braided channels are frequently associated with fish spawning activities, supporting higher densities of mature spawners and fish embryos during the spawning season (Boyer et al., 2017). Similarly, in natural canyon segments or artificially levee-constrained reaches, channel narrowing induces strong longitudinal velocity gradients, giving rise to pool-riffle sequences, where deep pools provide overwintering refugia for fish, while shallow riffles sustain abundant food resources (Floyd et al., 2009). However, in this study, channel morphologies characterized by bifurcation and narrowing did not yield ecological benefits for fish species diversity comparable to those observed at confluences. This finding indicates that the interplay between channel morphology and hydrodynamics governs habitat filters, such as flow velocity and substrate composition, which selectively structure fish assemblages adapted to local environmental conditions, whereas the pronounced habitat heterogeneity at confluences fosters greater fish species richness.

The present study provides direct empirical evidence of how confluence dynamics influence fish density and species diversity, particularly at the cascading confluence between the Yangtze River and Poyang Lake. Notably, distinct fish distribution patterns were observed between the mainstream and the tributary. In the Yangtze River, fish exhibited high density but relatively low species richness, whereas in Poyang Lake, species diversity was greater despite lower fish densities (Figure 10). This pattern aligns with findings from two previous field surveys conducted at the same confluence in 2021 (Yuan et al., 2023). A plausible explanation is that the mainstream is characterized by relatively homogeneous hydro-environmental conditions, including higher flow velocity, greater water depth, and a uniform substrate, which results in limited habitat diversity (Rice et al., 2006). However, the high concentration and availability of food resources enable a few dominant species to outcompete others, leading to high-density fish populations. In contrast, the tributary, with its greater habitat heterogeneity, resource partitioning, and isolation effects, supports a higher degree of species coexistence despite lower individual densities (Bouska et al., 2023). This contrast reflects the dynamic equilibrium of species diversity in large river systems, shaped by the interplay between habitat heterogeneity and competitive exclusion. The confluence integrates the high-density fish assemblages of the mainstream with the high species diversity characteristic of the tributary, promoting a synergistic enhancement of both fish density and species richness, with both reaching their regional peak within the core confluence area, defined as the CHEZ in this study (Figure 10). These findings are consistent with previous research identifying confluences as ecological hotspots in other large river basins worldwide, such as the Amazon and Mississippi Rivers (Benda et al., 2004; Nakajima et al., 2017). However, this enhancement effect was not sustained over long distances downstream, with the fish community structure downstream of the CHEZ gradually returning to pre-confluence levels. This pattern suggests that while confluences create localized biodiversity hotspots, their influence on community structure may be constrained by hydrological and hydro-sedimentary conditions at the confluence rather than exerting a cumulative impact across larger spatial scales (Fernandes et al., 2004).

The convergence of mainstream and tributary generates complex momentum and mass mixing mechanisms at confluences, leading to a complex flow structure and mixing processes (Yuan et al., 2022). The present study suggests the spatial extent of the CHEZ and its enhancement effect on fish communities are closely linked to the confluence hydrodynamic processes and mixing dynamics (Figure 10 & Table 3). Two distinct patterns of the CHEZ were identified in this study: when the momentum of the mainstream and tributary are roughly equivalent

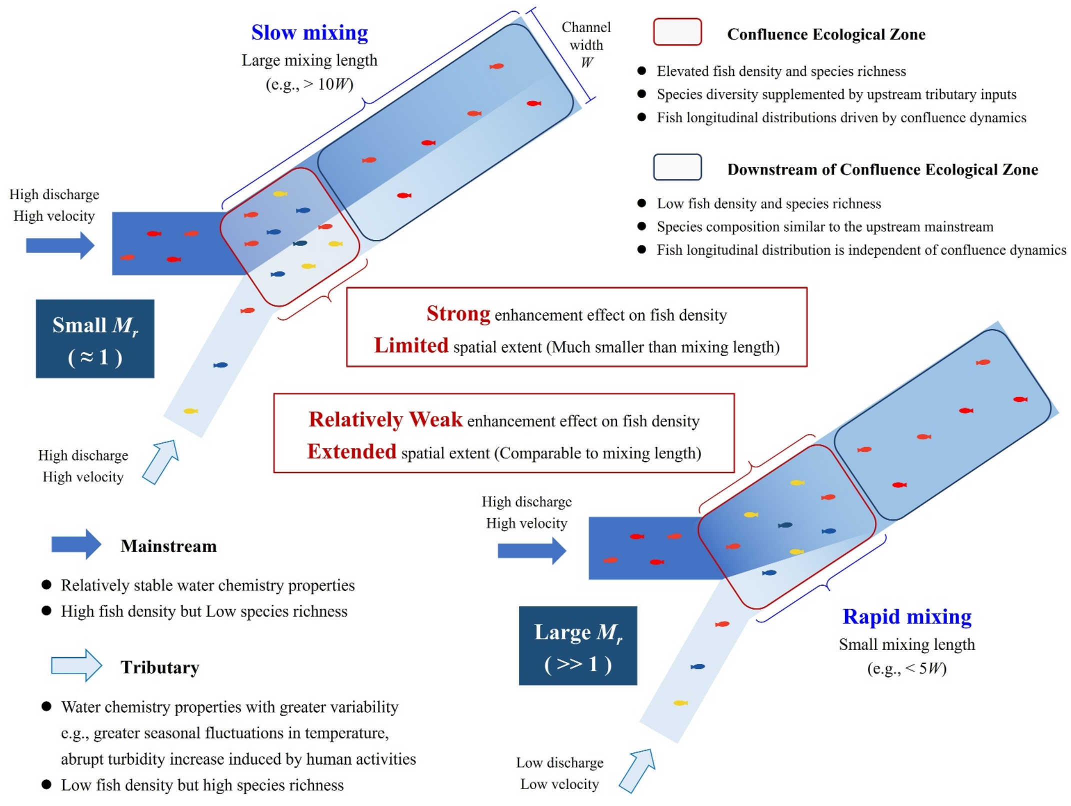


**Figure 10.** Conceptual model of fish distribution patterns driven by hydrodynamic processes and mixing dynamics at a river confluence and its downstream area. $M_r$ is the momentum ratio between the mainstream and tributary.

(Momentum ratio between the mainstream and tributary $M_r \approx 1$), slow mixing occurs between the two converging flows, with the mixing length extending over 10 times the width of the post-confluence channel. In this case, the CHEZ exerts a stronger enhancement effect on fish density, though its spatial extent is relatively limited. When the momentum of the mainstream greatly exceeds that of the tributary ($M_r >> 1$), mixing between the two flows was rapid, with the mixing length being lower than five times the channel width. Although the enhancement effect on fish density within the CHEZ was comparatively weaker, its spatial extent was larger, roughly corresponding to the mixing length. The observed difference in the effect and spatial extent of CHEZ might be due to the contrasting mixing dynamics regulated by momentum conditions: rapid mixing in the unequal momentum regime ($M_r >> 1$) facilitates the broad—scale dispersion of energy and materials, thereby spatially expanding the ecological effects, while slow mixing in the equivalent momentum regime ($M_r \approx 1$) preserves higher habitat heterogeneity, reinforcing localized ecological effects. Such interactions between hydrodynamics and ecological processes provide valuable insights into hydro-ecological synergistic design in ecological restoration. By regulating the discharge ratio between the mainstream and tributaries through hydraulic interventions, it is possible to actively define an optimal range for the momentum ratio at confluences, such as $0.8 < M_r < 1.2$ to improve fish habitat heterogeneity, or $M_r >> 1$ to facilitate fish longitudinal migration.

However, it is important to recognize that the momentum ratio is not the sole determinant of mixing dynamics. Xu et al. (2022) identified a similar correlation between the momentum ratio and mixing rate at the Yangtze River-Poyang Lake confluence (Table 3) but further emphasized that secondary flows and lock-exchange flows associated to the density effects also jointly modulate the mixing process. Lane et al. (2008) observed that at the large confluence of the Río Paraná and Río Paraguay, an exceptionally slow mixing process, with a mixing length exceeding 400 km, occurred at a momentum ratio of 3.6. This slow mixing was primarily due to the bed discordance at the confluence, which inhibited lateral exchange between the mainstem and the tributary.

Although complex habitat environments are generally favorable for fish communities, our study revealed that the initial confluence reach C1, which was characterized by the greatest variation in water quality parameters, attracted

**Table 3**
*Comparison of Confluence-Related Characteristics Observed in the Present Survey With Findings From Other Research Conducted at Large River Confluences*

| | | | | | | | Confluence hydro-ecological zone | |
|---|---|---|---|---|---|---|---|---|
| Survey area | | Survey time | Post-confluence channel width W (km) | Momentum ratio Mr | Mixing length L (km) | *L*:*W* | Enhancement effect | Length |
| The Yangtze River-Poyang Lake Confluence, China | The present study | April 2023 | 2.2 | 1 | >30 | >14 | 123% | >4 W |
| | | July 2023 | 2.3 | 3.6 | 12 | ~5 | 75% | ~5 W |
| | Xu et al. (2022) | August 2020 | 2.5 | 5.9 | Fast mixing (no specific numerical record) | | – | |
| | | December 2020 | 2 | 16.7 | Fastest mixing (no specific numerical record) | | | |
| | | April 2021 | 2.2 | 4.3 | Slow mixing (no specific numerical record) | | | |
| | | June 2021 | 2.4 | 0.8 | Slowest mixing (no specific numerical record) | | | |
| The Río Paraná-Río Paraguay Confluence, Argentina | Lane et al. (2008) | February 2004 | 2.8 | 1.8 | 8 | ~3 | – | |
| | | May 2005 | 2.8 | 3.6 | >400 | ~127 | | |

*Note.* The momentum ratio is defined as the ratio of the mainstream momentum to the tributary momentum. Due to the potential influence of seasonal population dynamics on the density of small-sized fish, the enhancement effect of the Confluence Hydro-Ecological Zone here refers to the average increase in the density of medium- and large-sized fish within it relative to the upstream mainstream.

predominantly small-sized fish in July, whereas larger fish concentrated slightly further downstream, for example, in reaches C2 and C3. This pattern may be attributed to the different hydrodynamic tolerance and habitat selection strategies of various sized fish. Small-sized fish are more strongly influenced by hydrodynamic forces, which cause them to disperse with the flow, whereas larger fish have a greater capacity to navigate and select more stable habitats downstream (Thornbrugh & Gido, 2010). Consequently, large fish were more frequently observed in the slightly farther downstream reaches, where habitat variability remains pronounced, but the flow field returned to relative stability, while small fish drifting from the upstream mainstream during the spawning season, were more strongly constrained by the complex flow structures in the initial confluence reach. Previous studies have shown similar size-dependent responses, with larger fish preferentially inhabiting areas where hydrodynamic variability is reduced (Gualtieri et al., 2020; Yuan et al., 2023). The presence of counter-rotating helical cells and shear layers within the confluence zone (Xu et al., 2022) may further influence fish habitat preferences, underscoring the necessity for more detailed investigations into fine-scale interactions between hydrodynamics and fish behavior.

These findings highlight the ecological significance of river confluences, particularly in human-modified and regulated river networks, where habitat fragmentation and flow regulation pose major challenges to fish populations. Confluences not only serve as biodiversity hotspots but also act as critical buffer zones that mitigate the impacts of upstream hydraulic modifications on downstream ecosystems (King, 2004; Makrakis et al., 2021; Shen et al., 2021, 2022). For instance, the high density of small-sized fish observed during the July survey underlines the role of confluences as essential nursery habitats during spawning seasons, like findings from the Amazon Basin (Cao et al., 2023; Fernandes et al., 2004). Additionally, confluences may provide thermal refugia for fish under climate change scenarios, as demonstrated in studies showing that cold-water tributary inputs can expand the habitat range of thermally sensitive species (Wang et al., 2020). However, the long-term ecological contributions of confluences remain uncertain due to their inherent dynamics. This study focused on two seasonal surveys, yet interannual variations in hydrological regimes, anthropogenic disturbances, and climate-driven changes in flow conditions could significantly alter confluence-mediated ecological processes. Future research should incorporate high-frequency monitoring, hydrodynamic modeling, and fish tracking technologies to better quantify the persistence of tributary effects across different temporal and spatial scales.

## 5. Conclusion

The present study investigated the large-scale hydrodynamic-ecological coupling mechanisms within the morphologically complex reach of the Yangtze River through two comprehensive field surveys conducted during critical spawning periods for local fish species in April and July, respectively. By integrating hydrodynamic and water quality measurements, hydroacoustic fish detections, and environmental DNA assessments, the primary aim was to quantify the spatiotemporal dynamics of fish communities and their responses to habitat drivers shaped by complex channel morphologies, with particular emphasis on the confluence-driven hydrodynamic processes and mixing dynamics. The key findings and implications are summarized as follows:

1. The morphically complex channel encompassing the Yangtze River-Poyang Lake cascading confluence and its downstream bifurcated and narrowing reaches, produce highly complex hydrodynamic processes and mixing dynamics, thereby shaping spatial and temporal patterns of heterogeneous fish distribution.
2. Tributary inflows further regulate the hydrodynamic and mixing processes within the morphologically complex channel: in April, when the discharges of the Yangtze River and Poyang Lake were comparable, the momentum ratio $M_r$ close to 1, resulting in slow mixing, with the mixing length exceeding 30 times the post-confluence channel width; whereas in July, when the Yangtze River discharge was nearly twice that of Poyang Lake, the intensified backwater effect led to an $M_r$ much greater than 1, facilitating complete mixing within approximately 12 times the channel width.
3. Among the channel morphological features, the first confluence of the cascading confluence system and the downstream narrowing reach exhibited the most pronounced enhancement in fish density. Especially, a distinct CHEZ was identified downstream of the first confluence, where fish density increased by as much as 150%. In contrast, the second confluence, involving two inflows with similar water quality properties, did not exhibit a comparable hotspot effect, likely due to the absence of significant water-quality contrast between the converging flows.
4. Rapid mixing in the unequal momentum regime ($M_r >> 1$) extended the spatial extent of the CHEZ, whereas slow mixing in the equivalent momentum regime ($M_r \approx 1$) strengthened the ecological effect within the CHEZ.
5. The density distribution of medium- and large-sized fish was primarily regulated by the water depth and the variability of water quality parameters in the post-confluence channel, whereas the density of small-sized fish was shaped by the combined effects of seasonal population dynamics and habitat heterogeneity.
6. Compared to other morphological components of the river system, confluences confer additional ecological benefits for biodiversity, as the input of tributary with high species diversity introduced localized biodiversity hotspots within the CHEZ, with species richness nearly twice that of the upstream mainstream; while downstream of the CHEZ, species richness declines to levels comparable to the upstream mainstream, accompanied by a similar species composition.

Insights from this study suggest that river management in morphologically complex reaches may benefit from a process-informed framework that considers the combined influence of hydrodynamic and water-quality conditions, and biological factors such as seasonal fish population dynamics. While hydrodynamic configuration (e.g., discharge and momentum ratios) plays a role in shaping ecological hotspots such as the CHEZ, its effectiveness is context-dependent and should be integrated with other environmental and ecological variables. This study provides a preliminary basis for understanding how channel morphology and associated processes influence ecological function, offering guidance for sustainable management of large river systems.

**Acknowledgments**
This research was funded by the National Key R&D Program of China (Grant 2022YFC3202602), the National Natural Science Foundation of China (Grant U2340221), Natural Science Foundation of Jiangsu Province (Grant BK20230036), and the 111 Project (Grant B17015). The authors acknowledge the contribution from 111 Project which funded the visits of Carlo Gualtieri at Hohai University in 2024. The authors also thank Hao Lin, Jiaming Yang, Fengyun Wan, An Wan, Pengxiang Cai of Hohai University for their support during the field surveys.

## Data Availability Statement

The raw data are available for download: https://zenodo.org/records/15120863.

## References

Abrial, E., Espinola, L. A., Amsler, M. L., Rabuffetti, A. P., Latosinski, F. G., Szupiany, R. N., et al. (2019). Fish structure in channel networks of a large anabranching floodplain: Effect of isolation/connection processes. *Water Resources Research*, *55*(12), 10993–11006. https://doi.org/10.1029/2019WR025063

Bean, C. W., Winfield, I. J., & Fletcher, J. M. (1996). *Stock assessment of the Arctic Charr (*Salvelinus alpinus*) population in Loch Ness, UK, Stock Assessment in Inland Fisheries*. Fishing News Books, Blackwell, Scientific Publications.

Belletti, B., de Leaniz, C. G., Jones, J., Bizzi, S., Boerger, L., Segura, G., et al. (2020). More than one million barriers fragment Europe's rivers. *Science*, *588*(7838), 436. https://doi.org/10.1038/s41586-020-3005-2

Benda, L. E., Poff, N. L., Miller, D., Dunne, T., Reeves, G., Pess, G., & Pollock, M. (2004). The network dynamics hypothesis: How channel networks structure riverine habitats. *BioScience*, *54*(5), 413–427. https://doi.org/10.1641/0006-3568(2004)054[0413:TNDHHC]2.0.CO;2

Best, J. L. (1987). Flow dynamics at river channel confluences: Implications for sediment transport and bed geomorphology. *Recent Developments in Fluvial Sedimentology*, *39*, 27–35. https://doi.org/10.2110/pec.87.39.0027

Boddy, N. C., Booker, D. J., & McIntosh, A. R. (2019). Confluence configuration of river networks controls spatial patterns in fish communities. *Landscape Ecology*, *34*(1), 187–201. https://doi.org/10.1007/s10980-018-0763-4

Bouska, K. L., Healy, B. D., Moore, M. J., Dunn, C. G., Spurgeon, J. J., & Paukert, C. P. (2023). Diverse portfolios: Investing in tributaries for restoration of large river fishes in the Anthropocene. *Frontiers in Environmental Science*, *11*, 1151315. https://doi.org/10.3389/fenvs.2023.1151315

Boyer, J. K., Guy, C. S., Webb, M., Horton, T. B., & McMahon, T. E. (2017). Reproductive ecology, spawning behavior, and juvenile distribution of mountain Whitefish in the Madison River, Montana. *Transactions of the American Fisheries Society*, *146*(5), 939–954. https://doi.org/10.1080/00028487.2017.1313778

Cao, J., Cheng, F., Wang, Z., Song, Y., & Xie, S. (2023). A "pulse-stairstep" longitudinal pattern of larval fish assemblages in a channelized floodplain river downstream of a dam: Dominant influences of major tributaries with a "confluence refuge concept". *Hydrobiologia*, *850*(18), 3981–3995. https://doi.org/10.1007/s10750-023-05281-9

Coley, A. R., & Clabburn, P. (2005). GIS visualisation and analysis of mobile hydroacoustic fisheries data: A practical example. *Fisheries Management and Ecology*, *12*(6), 361–367. https://doi.org/10.1111/j.1365-2400.2005.00461.x

Constantinescu, G., & Gualtieri, C. (2024). River confluences: A review of recent field and numerical studies. *Environmental Fluid Mechanics*, *24*(6), 1143–1191. https://doi.org/10.1007/s10652-024-10002-4

Constantinescu, G., Miyawaki, S., Rhoads, B., Sukhodolov, A., & Kirkil, G. (2011). Structure of turbulent flow at a river confluence with momentum and velocity ratios close to 1: Insight provided by an eddy-resolving numerical simulation. *Water Resources Research*, *47*(5). https://doi.org/10.1029/2010WR010018

Czegledi, I., Saly, P., Takacs, P., Dolezsai, A., Nagy, S. A., & Eros, T. (2016). The scales of variability of stream fish assemblage at tributary confluences. *Aquatic Sciences*, *78*(4), 641–654. https://doi.org/10.1007/s00027-015-0454-z

Dettmers, J., Wahl, D., Soluk, D., & Gutreuter, S. (2001). Life in the fast lane: Fish and foodweb structure in the main channel of large rivers. *Journal of the North American Benthological Society*, *20*(2), 255–265. https://doi.org/10.2307/1468320

Dudgeon, D., Arthington, A. H., Gessner, M. O., Kawabata, Z. I., Knowler, D. J., Leveque, C., et al. (2006). Freshwater biodiversity: Importance, threats, status and conservation challenges. *Biological Reviews*, *81*(2), 163–182. https://doi.org/10.1017/S1464793105006950

Egerton, J. P., Bolser, D. G., Grüss, A., & Erisman, B. E. (2021). Understanding patterns of fish backscatter, size and density around petroleum platforms of the U.S. Gulf of Mexico using hydroacoustic data. *Fisheries Research*, *233*, 105752. https://doi.org/10.1016/j.fishres.2020.105752

Fernandes, C. C., Podos, J., & Lundberg, J. G. (2004). Amazonian ecology: Tributaries enhance the diversity of electric fishes. *Science*, *305*(5692), 1960–1962. https://doi.org/10.1126/science.1101240

Floyd, T. A., Macinnis, C., & Taylor, B. R. (2009). Effects of artificial woody structures on Atlantic salmon habitat and populations in a Nova Scotia stream. *River Research and Applications*, *25*(3), 272–282. https://doi.org/10.1002/rra.1154

Fry, B. (2002). Stable isotopic indicators of habitat use by Mississippi River fish. *Journal of the North American Benthological Society*, *21*(4), 676–685. https://doi.org/10.2307/1468438

Gualtieri, C., Abdi, R., Ianniruberto, M., Filizola, N., & Endreny, T. A. (2020). A 3D analysis of spatial habitat metrics about the confluence of Negro and Solimoes rivers, Brazil. *Ecohydrology*, *13*(1), e2166. https://doi.org/10.1002/eco.2166

Gualtieri, C., Ianniruberto, M., & Filizola, N. (2019). On the mixing of rivers with a difference in density: The case of the Negro/Solimões confluence, Brazil. *Journal of Hydrology*, *578*(11), 124029. https://doi.org/10.1016/j.jhydrol.2019.124029

Hanfling, B., Handley, L. L., Read, D. S., Hahn, C., Li, J., Nichols, P., et al. (2016). Environmental DNA metabarcoding of lake fish communities reflects long-term data from established survey methods. *Molecular Ecology*, *25*(13), 3101–3119. https://doi.org/10.1111/mec.13660

Herrero, H. S., Diaz Lozada, J. M., Garcia, C. M., Szupiany, R. N., Best, J., & Pagot, M. (2018). The influence of tributary flow density differences on the hydrodynamic behavior of a confluent meander bend and implicationsfor flow mixing. *Geogeomorphology*, *304*, 99–112. https://doi.org/10.1016/j.geomorph.2017.12.025

Hu, M., Wu, Z., & Liu, Y. (2011). Time course of the juvenile major Chinese carps in the Hukou waters of Poyang Lake. *Resources and Environment in the Yangtze Basin*, *20*, 534–539.

Kenworthy, S. T., & Rhoads, B. L. (1995). Hydrologic control of spatial patterns of suspended sediment concentration at a stream confluence. *Journal of Hydrology*, *168*(1–4), 251–263. https://doi.org/10.1016/0022-1694(94)02644-Q

King, A. J. (2004). Ontogenetic patterns of habitat use by fishes within the main channel of an Australian floodplain river. *Journal of Fish Biology*, *65*(6), 1582–1603. https://doi.org/10.1111/j.0022-1112.2004.00567.x

Lane, S. N., Parsons, D. R., Best, J. L., Orfeo, O., Kostaschuk, R. A., & Hardy, R. J. (2008). Causes of rapid mixing at a junction of two large rivers: Río Paraná and Río Paraguay, Argentina. *Journal of Geophysical Research*, *113*(F2), F02019. https://doi.org/10.1029/2006jf000745

Liu, Y., Yang, X., Ren, P., Li, X., Fang, D., & Xu, D. (2019). Community characteristics of larvae and juvenile fish in Hukou section of the Yangtze River in spring and summer. *Acta Hydrobiologica Sinica*, *43*, 142–154. https://doi.org/10.7541/2019.018

Makrakis, M. C., Refatti, A., Keckeis, H., Silva, P. S., Assumpcao, L., Kashiwaqui, E. A. L., et al. (2021). Importance of a turbulent river section below a giant waterfall for fish spawning: Indications from drift and dispersion patterns of early life stages. *Ecohydrology*, *15*(1), e2356. https://doi.org/10.1002/eco.2356

Meem, T. H., Rhoads, B. L., Lewis, Q. W., Umar, M., & Sukhodolov, A. (2025). Length scales, rates, and variability of mixing downstream of river confluences. *Geophysical Research Letters*, *52*(8), e2025GL114640. https://doi.org/10.1029/2025GL114640

Nagayama, S., & Nakamura, F. (2018). The significance of meandering channel to habitat diversity and fish assemblage: A case study in the Shibetsu river, northern Japan. *Limnology*, *19*(1), 7–20. https://doi.org/10.1007/s10201-017-0512-4

Nakajima, R., Rimachi, E. V., Santos-Silva, E. N., Calixto, L. S. F., Leite, R. G., Khen, A., et al. (2017). The density and biomass of mesozooplankton and ichthyoplankton in the Negro and the Amazon Rivers during the rainy season: The ecological importance of the confluence boundary. *PeerJ*, *5*, e3308. https://doi.org/10.7717/peerj.3308

Polvi, L. E., Lind, L., Persson, H., Miranda-Melo, A., Pilotto, F., Su, X., & Nilsson, C. (2020). Facets and scales in river restoration: Nestedness and interdependence of hydrological, geomorphic, ecological, and biogeochemical processes. *Journal of Environmental Management*, *265*, 110288. https://doi.org/10.1016/j.jenvman.2020.110288

Pouchoulin, S., LeCoz, J., Mignot, E., Gond, L., & Riviere, N. (2020). Predicting transverse mixing efficiency downstream of a river confluence. *Water Resources Research*, *56*(10), e2019WR026367. https://doi.org/10.1029/2019WR026367

Qiu, J., Yuan, S., Tang, H., Zhang, Q., Wolter, C., & Nikora, V. (2024). Ecological connectivity of river-lake ecosystem: Evidence from fish population dynamics in a connecting channel. *Water Resources Research*, *60*(10), e2024WR037495. https://doi.org/10.1029/2024WR037495

Rhoads, B. L., & Johnson, K. K. (2018). Three-dimensional flow structure, morphodynamics, suspended sediment, and thermal mixing at an asymmetrical river confluence of a straight tributary and curving main channel. *Geogeomorphology*, *323*, 51–69. https://doi.org/10.1016/j.geomorph.2018.09.009

Rhoads, B. L., Schwartz, J. S., & Porter, S. A. (2003). Stream geomorphology and variability of hydraulic habitat for fish in four Midwestern agricultural streams. *Water Resources Research*, *39*(8), 1218. https://doi.org/10.1029/2003WR002294

Rice, S. P., Ferguson, R. I., & Hoey, T. B. (2006). Tributary control of physical heterogeneity and biological diversity at river confluences. *Canadian Journal of Fisheries and Aquatic Sciences*, *63*(11), 2553–2566. https://doi.org/10.1139/F06-145

Riley, J. D., & Rhoads, B. L. (2012). Flow structure and channel geomorphology at a natural confluent meander bend. *Geogeomorphology*, *163*, 84–98. https://doi.org/10.1016/j.geomorph.2011.06.011

Shen, X., Hodges, B. R., Li, R., Li, Z., Fan, J., Cui, N., & Cai, H. (2021). Factors influencing distribution characteristics of total dissolved gas supersaturation at confluences. *Water Resources Research*, *57*(6). https://doi.org/10.1029/2020WR028760

Shen, X., Li, R., Cai, H., Feng, J., & Wan, H. (2022). Characteristics of secondary flow and separation zone with different junction angle and flow ratio at river confluences. *Journal of Hydrology*, *614*, 128537. https://doi.org/10.1016/j.jhydrol.2022.128537

Song, Y., Cheng, F., Murphy, B. R., & Xie, S. (2018). Downstream effects of the Three Gorges Dam on larval dispersal, spatial distribution, and growth of the four major Chinese carps call for reprioritizing conservation measures. *Canadian Journal of Fisheries and Aquatic Sciences*, *75*(1), 141–151. https://doi.org/10.1139/cjfas-2016-0278

Thornbrugh, D. J., & Gido, K. B. (2010). Influence of spatial positioning within stream networks on fish assemblage structure in the Kansas River basin, USA. *Canadian Journal of Fisheries and Aquatic Sciences*, *67*(1), 143–156. https://doi.org/10.1139/F09-169

Vannote, R. L., Minshall, G. W., Cummins, K. W., Sedell, J. R., & Cushing, C. E. (1980). The river continuum concept. *Canadian Journal of Fisheries and Aquatic Sciences*, *37*(1), 130–137. https://doi.org/10.1139/F80-017

Wang, N., Liu, S., Guo, X., Li, Z., Cong, N., Bao, M., et al. (2025). The impact of channel sinuosity and hydrodynamics on fish-habitat suitability in high-gradient meandering rivers. *Ecological Engineering*, *215*, 107586. https://doi.org/10.1016/j.ecoleng.2025.107586

Wang, T., Kelson, S., Greer, G., Thompson, S., & Carlson, S. M. (2020). Tributary confluences are dynamic thermal refuges for a juvenile salmonid in a warming river network. *River Research and Applications*, *36*(7), 1076–1086. https://doi.org/10.1002/rra.3634

Xu, L., Yuan, S., Tang, H., Qiu, J., Xiao, Y., Whittaker, C., & Gualtieri, C. (2022). Mixing dynamics at the large confluence between the Yangtze River and Poyang Lake. *Water Resources Research*, *58*(11), e2022WR032195. https://doi.org/10.1029/2022WR032195

Yuan, S., Qiu, J., Tang, H., Xu, L., Xiao, Y., Liu, M., et al. (2023). Fish community traits near a large confluence: Implications for its nodal effects in the river ecosystem. *Journal of Hydrology*, *626*(2023), 130335. https://doi.org/10.1016/j.jhydrol.2023.130335

Yuan, S., Tang, H., Li, K., Xu, L., Xiao, Y., Gualtieri, C., et al. (2021). Hydrodynamics, sediment transport and geomorphological features at the confluence between the Yangtze river and the Poyang Lake. *Water Resources Research*, *57*(3), e2020WR028284. https://doi.org/10.1029/2020WR028284

Yuan, S., Xu, L., Tang, H., Xiao, Y., & Gualtieri, C. (2022). The dynamics of river confluences and their effects on the ecology of aquatic environment: A review. *Journal of Hydrodynamics*, *34*, 1–14. https://doi.org/10.1007/s42241-022-0001-z

Yuan, S., Zheng, Y., Tang, H., Chen, Y., Xu, L., Whittaker, C., & Gualtieri, C. (2024). Large wood transport and accumulation near the separation zone of a channel confluence. *Water Resources Research*, *60*(3), e2023WR034790. https://doi.org/10.1029/2023WR034790

Zhou, X., Xu, M., Lei, F., Zhang, J., Wang, Z., & Luo, Y. (2022). Responses of macroinvertebrate assemblages to flow in the Qinghai-Tibet Plateau: Establishment and application of a multi-metric habitat suitability model. *Water Resources Research*, *58*(5), e2021WR030909. https://doi.org/10.1029/2021WR030909